Article

Comprehensive Passive Thermal Management Systems for Electric Vehicles

Hamidreza Behi [1,2,*] **, Danial Karimi** [1,2] **, Rekabra Youssef** [1,2] **, Mahesh Suresh Patil** [1,2] **, Joeri Van Mierlo** [1] **and Maitane Berecibar** [1]

1   Research Group MOBI—Mobility, Logistics, and Automotive Technology Research Centre,
    Vrije Universiteit Brussel, Pleinlaan 2, 1050 Brussels, Belgium; Danial.Karimi@VUB.be (D.K.);
    Rekabra.Youssef@vub.be (R.Y.); Mahesh.Suresh.Patil@vub.be (M.S.P.); Joeri.Van.Mierlo@vub.be (J.V.M.);
    Maitane.Berecibar@vub.be (M.B.)
2   Flanders Make, 3001 Heverlee, Belgium
*   Correspondence: Hamidreza.Behi@VUB.be; Tel.: +32-(0)26292838

Abstract: Lithium-ion (Li-ion) batteries have emerged as a promising energy source for electric vehicle (EV) applications owing to the solution offered by their high power, high specific energy, no memory effect, and their excellent durability. However, they generate a large amount of heat, particularly during the fast discharge process. Therefore, a suitable thermal management system (TMS) is necessary to guarantee their performance, efficiency, capacity, safety, and lifetime. This study investigates the thermal performance of different passive cooling systems for the LTO Li-ion battery cell/module with the application of natural convection, aluminum (Al) mesh, copper (Cu) mesh, phase change material (PCM), and PCM-graphite. Experimental results show the average temperature of the cell, due to natural convection, Al mesh, Cu mesh, PCM, and PCM-graphite compared with the lack of natural convection decrease by 6.4%, 7.4%, 8.8%, 30%, and 39.3%, respectively. In addition, some numerical simulations and investigations are solved by COMSOL Multiphysics®, for the battery module consisting of 30 cells, which is cooled by PCM and PCM-graphite. The maximum temperature of the battery module compared with the natural convection case study is reduced by 15.1% and 17.3%, respectively. Moreover, increasing the cell spacing in the battery module has a direct effect on temperature reduction.

Keywords: lithium-ion battery; thermal management system; natural convection; aluminum mesh; copper mesh; phase change material

1. Introduction

Global warming and air pollution have pushed researchers to replace a clean alternative source for fossil fuels [1,2]. Transportation is one of the main consumers which is related to fossil fuels. Electric vehicles (EVs) and hybrid electric vehicles (HEVs) with low CO_2 emissions are the most appropriate alternatives for conventional vehicles. Lithium-ion (Li-ion) batteries are the most promising energy source for EVs and HEVs owing to their features comprising high specific energy, high capacity, high power, and no memory effect [3–6]. Nonetheless, Li-ion batteries produce a noticeable amount of heat, particularly during the fast charging/discharge process. Consequently, the design and build of a suitable thermal management system (TMS) are vital to preserving the battery temperature in a safe temperature range (25–40 °C) [7]. TMSs are generally divided into active and passive cooling systems. Active cooling systems like forced air and liquid and refrigerant cooling systems [8] need an external source of energy. However, passive cooling systems like phase change material (PCM) [9,10], natural convection, heat sink [11], heat exchangers [12], fin, and heat pipe [13–15] do not consume any energy [16].

The air cooling [16–20] and liquid cooling [21–23] systems are common active cooling systems that can afford effective cooling for the Li-ion batteries. However, air cooling

systems are not practical in stressful conditions, due to the low thermal conductivity of air and the liquid cooling systems are huge, expensive, and fundamentally work with the high investment cost. Heat pipes are classified as passive cooling systems which suffer from complex design and severe operating environment requirements [24]. The main feature of the PCM is the absorption or release of the enormous amount of energy during the phase change process. The PCM-based TMSs are successful cooling systems with advantages in temperature control performance, simple layout, and no power consumption [25].

PCM is also combined by nanoparticle [26–29], heat pipe [13], fin, and mesh [30,31] because of its thermal properties. The concept of PCM for battery cooling was initially used by Al-Hallaj and Selman [32]. Babapoor et al. [33] studied the cooling performance of the carbon fiber-PCM composites on Li-ion batteries. They experimentally found a mixture of PCM with 2-mm-long carbon fibers and a mass percentage of 0.46%, which can decrease the maximum temperature of the battery simulator by up to 45%. Karimi et al. [31] experimentally and numerically investigated the effect of PCM and Al-mesh on Lithium-ion capacitors (LiC). They found that the PCM and Al-mesh can decrease the LiC temperature by 20%. Wang et al. [34] experimentally studied the effect of PCM on cylindrical battery packs under different discharge rates (1C, 2C). They found the PCM cooling method can meaningfully decrease the average temperature and improve the temperature uniformity of the Li-ion battery pack. Huang et al. [35] experimentally considered the effect of PCM-based TMS for the cylindrical battery module. They discovered that the proposed cooling system can control the temperature of the cylindrical battery module under 1C, 2C, and 3C discharging rates. Weng et al. [36] optimized the effect of PCM fin TMS for cylindrical cells in 1C and 2C discharging rates. They considered the strength of different fin shapes in specific applications. Behi et al. [37] investigated the cooling effectiveness of the PCM-assisted heat pipe on cell level. They could provide a 17.3% and 40.7% temperature reduction by heat pipe and PCM-assisted heat pipe cooling system. El Idi et al. [38] experimentally and numerically investigated a PCM metal foam composite for 18,650 cylindrical cells in 1.5C, 2.5C, and 4.5C rates. They found usage of Al foam improves the efficiency of the thermal management system.

According to recent studies, most of the research in low current profiles and C rates are cooled by passive cooling systems. To the authors' knowledge, the passive TMS for Li-ion batteries has been rarely addressed in the high current applications. In this study, natural convection, aluminum (Al) mesh, copper (Cu) mesh, PCM, and PCM-graphite have been considered on the LTO cell/module at the 8C discharging rate (184A). According to the results, the temperature of the cell has been decreased by 6.4%, 7.4%, 8.8%, 30%, and 39.3%, respectively, by natural convection, Al mesh, Cu mesh, PCM, and PCM-graphite compare with the lack of natural convection. For the battery module consisting of 30 cells that cooled through PCM and PCM-graphite, the maximum temperature compares with natural convection reduced by 15.1% and 17.3%, respectively. Moreover, some investigations are done to consider the effect of cell spacing. It is found by increasing the cell spacing from 0 to 8 mm, the maximum temperature of the module reduces by 13% and 13.7% for PCM and PCM-graphite, respectively.

2. Experimental Setup

The experimental setup is built to investigate the effect of passive cooling methods on the thermal management of the LTO battery cell. The key features of the prismatic LTO cell are presented in Table 1.

Table 1. The key data of the cell adapted from [37].

Factor	Value
Chemistry	LTO
Shape	Prismatic
Nominal voltage (V)	2.3
Capacity (Ah)	23
Specific energy (Wh/kg)	96
Energy density (Wh/L)	202
Weight (kg)	0.550
Volume (L)	0.260
Dimensions L × W × H (mm)	115 × 22 × 103
Heat specific capacity (J/kg·K)	1150
Thermal conductivity x,y,z (W/m·K)	31, 0.8, 31

In the experimental section, the performance of natural convection, Al and Cu mesh, PCM, and PCM-graphite has been considered on the cell level. The image of the test setup and the location of thermocouples are exposed in Figure 1. The experimental test setup included a tester, a cell, a Pico USB TC-08 data logger, four K-type thermocouples, and a personal computer. The accuracy of the thermocouples is around ±0.2 °C which are connected to the surface of the cell. It is important to note that the ambient temperature is set at 22 °C for all the tests, and T_4 is responsible for measuring it.
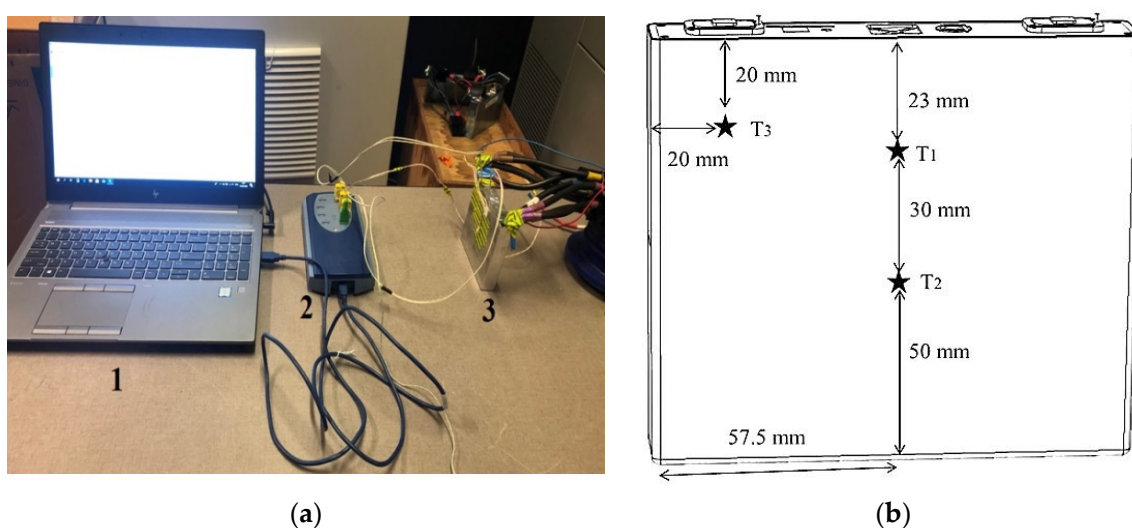

(**a**)   (**b**)

Figure 1. (**a**). The image of the experimental system comprising of (1) a personal computer; (2) data logger; (3) prismatic cell; and (**b**) the location and dimension of the thermocouples on the cell surface.

The battery tester (PEC) is used to start cycling. The PEC tester controls the cycling and records the voltage and current of the cell. The temperature of the cell is recorded by the external thermocouples. The discharging process is done under the current rate of 8C (184 A) at 446 s. The heat production of the cell can be calculated based on the following equation:

$$mC_p \frac{\partial T}{\partial t} + q_{conv} = k_x \frac{\partial^2 T}{\partial x^2} + k_y \frac{\partial^2 T}{\partial y^2} + k_z \frac{\partial^2 T}{\partial z^2} + q_g \tag{1}$$

According to Equation (1) m, cp, T, k, and q_g signify the mass, heat capacity, temperature, thermal conductivity, and heat production of the cell, respectively.

2.1. Experimental Results and Discussion

2.1.1. Lack and Presence of Natural Convection

The influence of the natural convection cooling method is the initial phase to consider for thermal management. The natural convection cooling condition refers to a passive cooling system that does not consume any external energy. The goal of this section is to find out the consequence of the natural convection on the heat production of the LTO cell at the 8C discharging process, which is capable of preparing specific guidance for battery cooling to compare with other cooling methods. The temperature of the cell in the discharging process and pictures of the tested battery in the presence and lack of natural convection are illustrated in Figure 2. As it is obvious the natural convection has a minor effect on the temperature trends of the thermocouples. According to the calculation, the heat transfer coefficient is considered 6.87 W/m^2 K [18]. The average temperature of the cell at the end of the discharging process in the lack and presence of the natural convection reaches 57.2 °C and 53.5 °C, which show a 6.4% reduction.

(a)

(b)

(c)

(d)
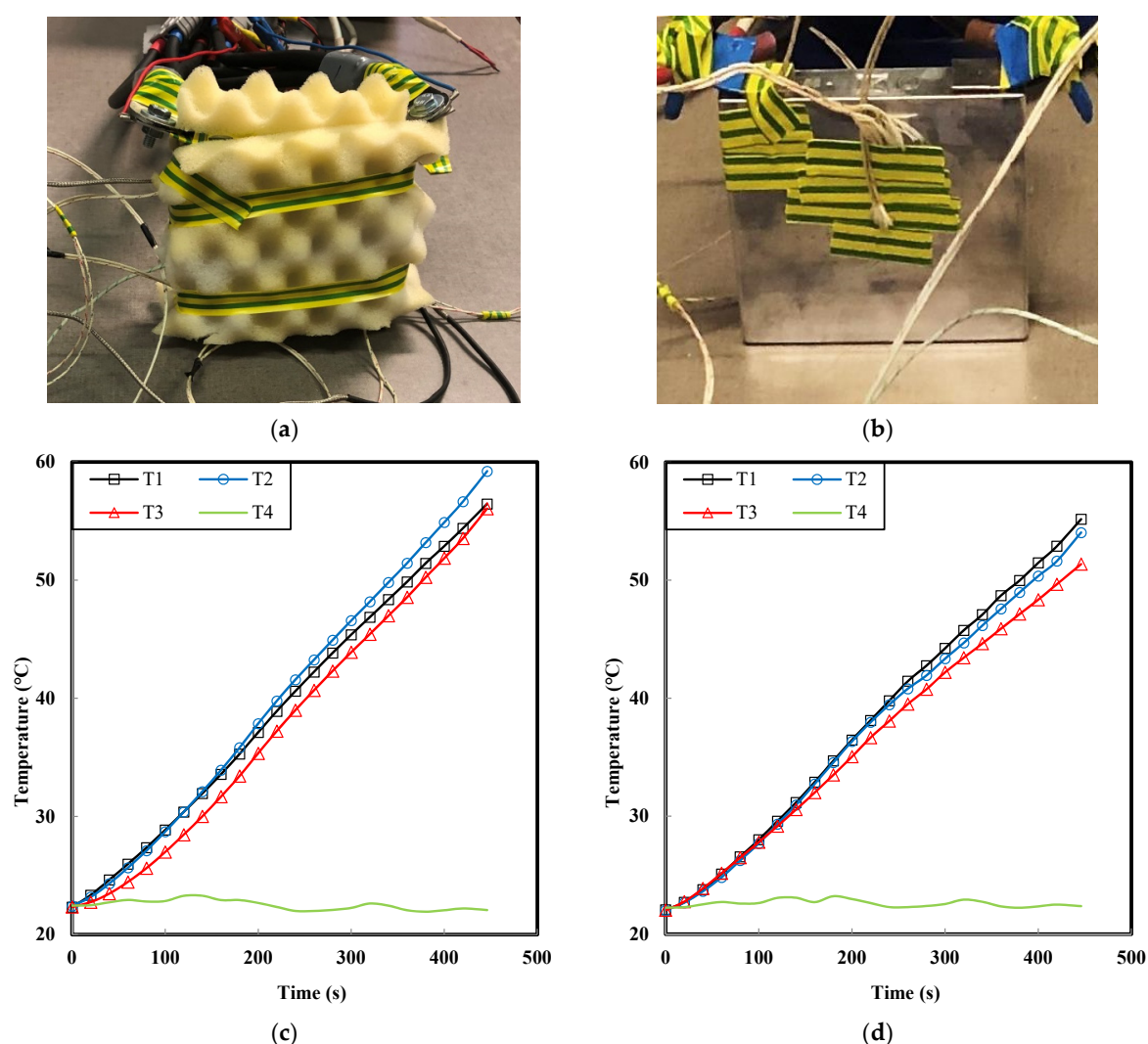
Figure 2. The image of the cell in (**a**) lack and (**b**) the presence of the natural convection and temperature curves in (**c**) lack and (**d**) the presence of the natural convection under the 8C discharging rate at 446 s.

2.1.2. Natural Convection Effect on Al and Cu Mesh

In this section, the effect of Al and Cu mesh on the temperature of the LTO cell in the presence of the natural convection has been considered. The metal mesh is a kind of heat sink classified as a passive heat exchanger that transfers heat generated by the battery to

air as a fluid medium. The Al and Cu mesh is classified as a passive heat sink that benefits high reliability and low-cost characters. It can be seen in Figure 3 that the temperature of the cell has been uniformed, due to Al and Cu mesh. Moreover, the average temperature of the cell wrapped with Al and Cu mesh at the end of the discharging process reaches 52.9 °C and 52.1 °C, which show a 7.4% and 8.8% reduction compared with the lack of natural convection.
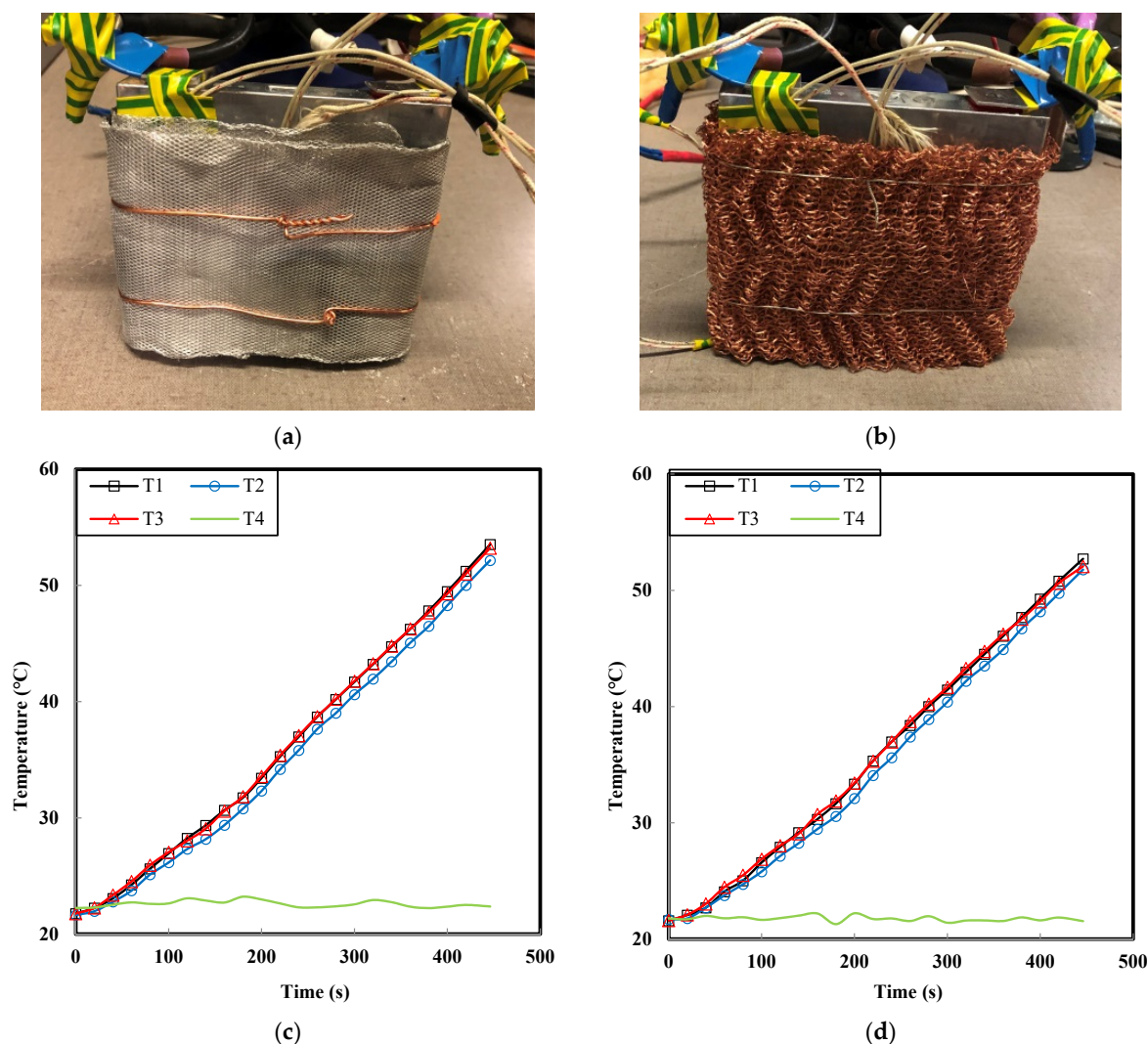

Figure 3. The picture of the cell embedded with the (**a**) Al mesh and (**b**) Cu mesh and temperature curves of (**c**) Al mesh (**d**) Cu mesh in the presence of the natural convection under the 8C discharging rate at 446 s.

2.1.3. PCM and PCM-Graphite Cooling

PCMs are using as an operational means of passive cooling in battery thermal management applications. Generally, PCM is named as a material that can store/release a huge amount of energy at a constant temperature or in a negligible temperature range during the phase change process. The usage of the PCMs is growing, owing to the effective features in temperature control and free energy consumption. In this study, for thermal management of the LTO cell, a PCM with a phase change temperature of 30 °C is chosen. The key data of the PCM and container are shown in Table 2. The utilized PCM in this study is organic paraffin wax, which is appropriate and operative for the suggested operating temperature range of the Li-ion battery cells.

Table 2. The key data of the PCM [37].

Parameter	Value
Melting point (°C)	25–32
Heat storage capacity (kJ/kg)	220
Specific heat capacity (kJ/kg K)	2.5
Density at 15 °C (kg/L)	0.8
Density at 80 °C (kg/L)	0.85
Thermal conductivity-solid (W/m·K)	0.25
Thermal conductivity-liquid (W/m·K)	0.4
Container thickness (mm)	8
Container dimensions (L × W × H) (mm)	130 × 40 × 105

According to Figure 4, the temperature of the cell is effectively controlled by the PCM in a safe temperature range (25–40 °C). The average temperature of the cell at the end of the discharging process in the presence of the PCM reaches 39.98 °C, which shows a 30% reduction compare with the lack of natural convection.
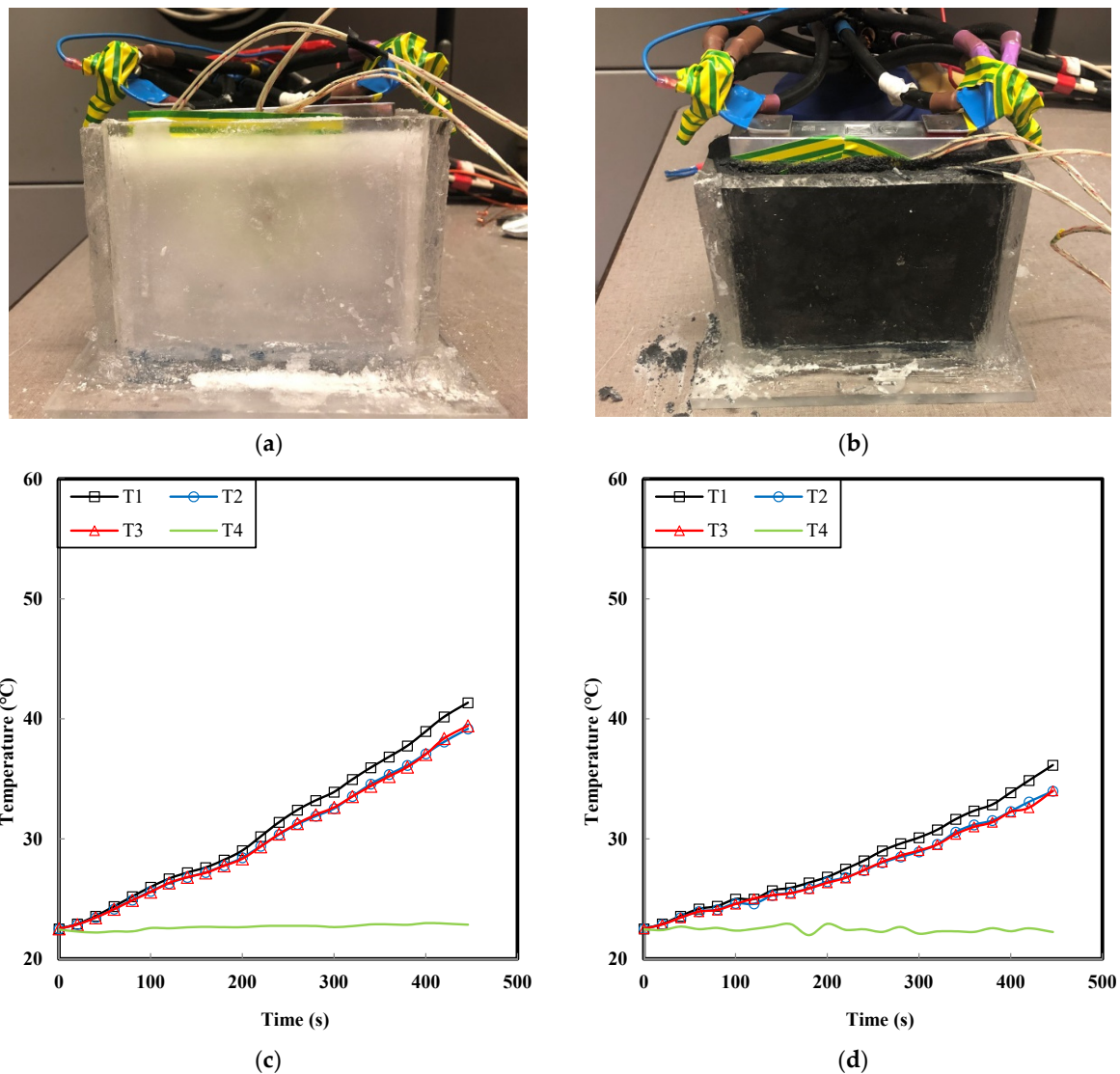

Figure 4. The picture of the cell embedded with the (**a**,**b**) PCM and PCM-graphite and the temperature curves (**c**,**d**) in the presence of the PCM and PCM-graphite under the 8C discharging rate at 446 s.

Nevertheless, most PCMs suffer from low thermal conductivity in energy storage and cooling applications [13,39–41]. Therefore, several approaches like adding nanoparticles, graphite, nanocarbon tube, and heat pipes are used to reimburse for this problem. In order to increase the cooling capability and thermal conductivity, porous graphite is added to the PCM. The main parameters of the PCM-graphite are mentioned in Table 3.

Table 3. The main properties of the PCM-graphite.

Parameter	Value
Melting point (°C)	25–32
Heat storage capacity (kJ/kg)	210
Specific heat capacity (kJ/kg·K)	2.5
Density at 15 °C (kg/L)	0.71
Density at 80 °C (kg/L)	0.75
Thermal conductivity-solid (W/m·K)	0.5
Thermal conductivity-liquid (W/m·K)	1
Container thickness (mm)	8
Container dimension (L × W × H) (mm)	130 × 40 × 105

To consider the cooling efficiency of the PCM-graphite, the Li-ion battery cell is directly submerged in the composite. The thermal contact resistance is extremely decreased via the submerged method, leading to higher cooling performance [42]. As is expected, the PCM-graphite displays a better cooling performance, due to higher thermal conductivity. The PCM composite gets benefitted from the high thermal conductivity of graphite and with a worthy heat storage capacity of the PCM. Figure 4d displays the performance of the PCM-graphite. The average cell temperature reaches 34.71 °C, which experiences 39.3% compared with the lack of natural convection.

2.1.4. Comparison Results

The value of the different passive cooling systems on the average temperature of the LTO cell is shown in Figure 5. In the same initial conditions, the average temperature of the cell in lack of natural convection, natural convection, Al mesh, Cu mesh, PCM, and PCM-graphite reaches the 57.24 °C, 53.52 °C, 52.96 °C, 52.18 °C, 39.98 °C, and 34.71 °C, respectively. As can be seen, PCM and PCM-graphite preserve the cell in the safe operating temperature range, which is shown by the dashed line.
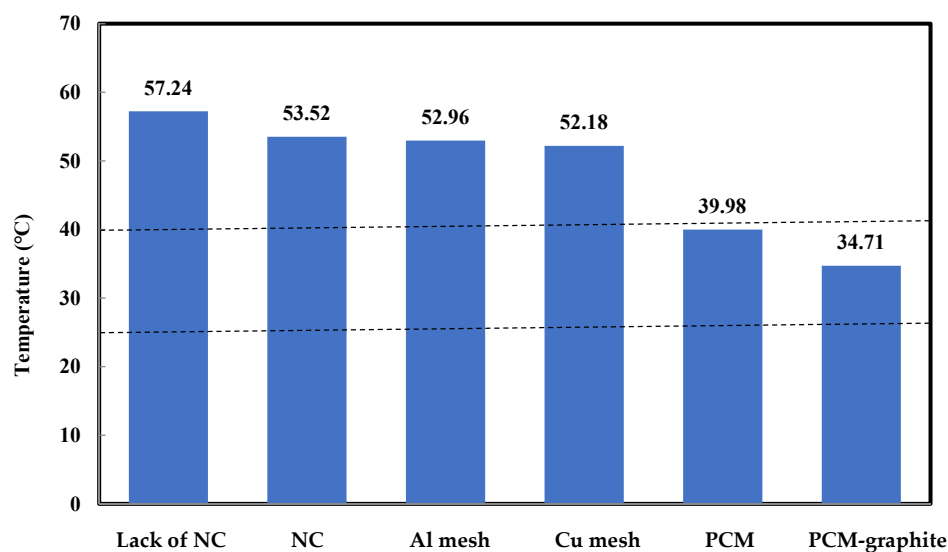

Figure 5. The comparison of the different passive cooling systems for LTO cell in the 8C discharging rate (NC = Natural convection).

3. Simulation

3.1. Battery Thermal Modeling

Matlab/Simulink (MathWorks, Natick, MA, USA) with COMSOL Multiphysics®
(COMSOL, Stockholm, Sweden) has been used to build the 3D thermal behavior of the
cell. Energy balance (Equation (1)) is utilized to describe the transient thermal genera-
tion inside the cell. In the current study, the heat production of the cell is calculated by
Matlab/Simulink from the ohmic resistance of the cell. Therefore, an electrical model of
the cell is built and validated with the dual-polarization electric-equivalent-circuit (ECM)
approach [43]. Figure 6 displays the recommended impedance model where Voc, R0, and
Vbatt present the open-circuit voltage, the series-connected ohmic resistance, and battery
terminal voltage, respectively. It also shows two parallel R//C branches, which represent
the time-dependent polarization processes.

$$q_g = R_{bt} \cdot I^2 + R_1 \cdot I_1{}^2 + R_2 \cdot I_2{}^2 \tag{2}$$

$$\dot{q} = R_{tab} \cdot I^2 \tag{3}$$

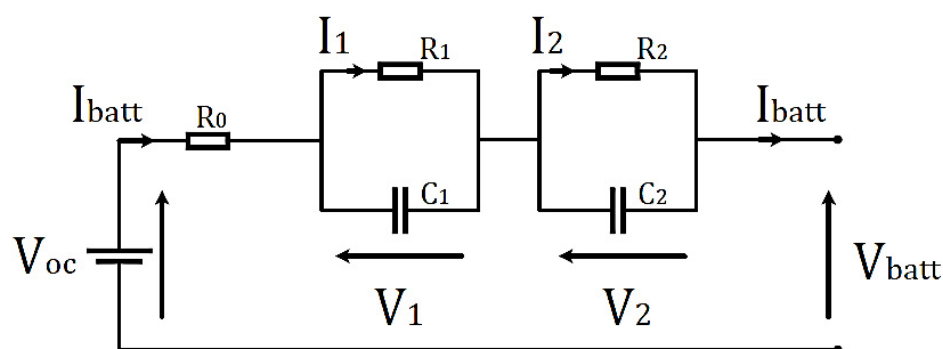$$R_{tab} = \rho' \frac{l}{S} \tag{4}$$

Figure 6. Equivalent impedance model of the cell adapted from [18].

Moreover, heat production of the tab domain is presented by Equation (3) [44]. Based
on the above equations, I and R_{bt} signify the current and ohmic resistance of the cell. In
addition, for the tab domains R_{tab}, ρ', l, and S are the electrical resistance, resistivity, length,
and cross-section of the corresponding tab, respectively. The convective heat transfer to the
ambient is also calculated as follows [45]:

$$q_{conv} = hS(T_{amb} - T_{bt}) \tag{5}$$

wherein, h and S signify the heat transfer coefficient and cross-section area of the cell.
Additionally, T_{bt} and T_{amb} determine the cell and ambient temperature.

3.2. Illustrative Equations for PCM

The governing equations for PCM comprising continuity, momentum, and energy
equations can be written as follows [13]:

$$\frac{\partial u_r}{\partial r} + \frac{u_r}{r} + \frac{\partial u_z}{\partial z} = 0 \tag{6}$$

$$\frac{\partial u_r}{\partial t} + u_r \frac{\partial u_r}{\partial r} + u_z \frac{\partial u_z}{\partial z} = -\frac{1}{\rho} \frac{\partial p}{\partial r} + \nu \left(\frac{\partial^2 u_r}{\partial r^2} + \frac{1}{r} \frac{\partial u_r}{\partial r} - \frac{u_r}{r^2} + \frac{\partial^2 u_r}{\partial z^2} \right) \tag{7}$$

$$\frac{\partial u_z}{\partial t} + u_r \frac{\partial u_z}{\partial r} + u_z \frac{\partial u_z}{\partial z} = -\frac{1}{\rho} \frac{\partial p}{\partial z} + \nu \left(\frac{\partial^2 u_z}{\partial r^2} + \frac{1}{r} \frac{\partial u_z}{\partial r} - \frac{u_r}{r^2} + \frac{\partial^2 u_z}{\partial z^2} \right) + g[\beta(T - T_m) - 1] \tag{8}$$

$$\frac{\partial h}{\partial t} + u_r \frac{\partial h}{\partial r} + u_z \frac{\partial h}{\partial z} = \frac{1}{\rho}\left[\frac{1}{r}\frac{\partial}{\partial r}\left(kr\frac{\partial T}{\partial r}\right) + \frac{\partial}{\partial z}\left(k\frac{\partial T}{\partial z}\right)\right] \tag{9}$$

where in u, T_1, T_m, T_2 and k present the velocity, initial temperature, melting temperature, the final temperature $(T_2 = T_m + \Delta T)$ and thermal conductivity of the PCM, respectively. Between the solid and liquid phases, a transition happens within the interval of ΔT which is named the mushy phase. The different phases of the PCM are as follows [37].

$$
\begin{aligned}
T^* \leq T_1 & \quad (Solid\ phase) \\
T_1 < T^* < T_2 & \quad (Mushy\ phase) \\
T^* \geq T_2 & \quad (Liquid\ phase)
\end{aligned}
\tag{10}
$$

The heat capacity and the thermal conductivity of the PCM can be mentioned as follows (s, solid; t, transition; l, liquid):

$$
C = \begin{cases} c_s & T^* \leq T_1 \\ c_t & T_1 < T^* < T_2 \\ c_l & T^* \geq T_2 \end{cases}
\tag{11}
$$

$$
k = \begin{cases} k_s & T^* \leq T_1 \\ \frac{k_s + k_l}{2} & T_1 < T^* < T_2 \\ k_l & T^* \geq T_2 \end{cases}
\tag{12}
$$

The total energy that can be stored in the PCM is calculated using the below equation:

$$Q_{PCM} = mc_s(T_1 - T_m) + mL + mc_l(T_2 - T_m) \tag{13}$$

where m represents the mass of the PCM. Totally, COMSOL by the revealed equations simulates the melting of the PCM allowing for conductive and convective heat transfer [46].

3.3. Validation of the Thermal Model for Natural Convection, PCM and PCM-Graphite

The experimental results for the 23Ah LTO cell at 8C discharging rate and initial temperature of 22 °C are validated under the effect of natural convection, PCM, and PCM-graphite with the COMSOL Multiphysics®. Four thermocouples are used experimentally to record the battery surface and ambient temperature, respectively. For validation, the T_1 thermocouple (Figure 1b) is selected for comparison with the experimental results. According to Figure 7, the difference between the simulation and experimental results for T_1 is in an acceptable range. The average relative errors for T_1 thermocouple, for states of a, b, and c are 4.6%, 1%, and 4.1%, respectively, within a standard error range less than 5% [47].
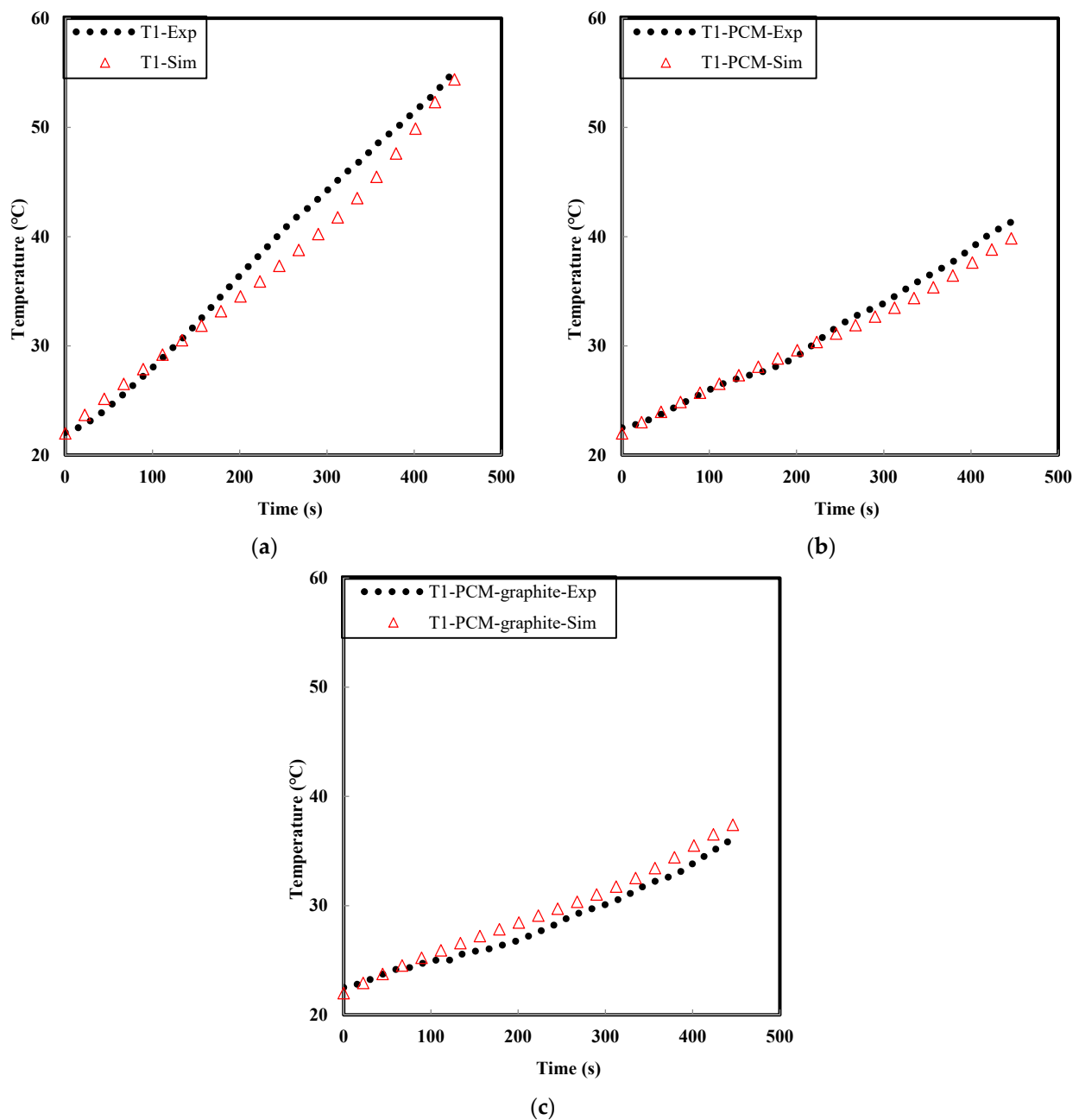
Figure 7. Thermal model validation of T_1 thermocouple in the presence of the (**a**) natural convection, (**b**) PCM, and (**c**) PCM-graphite under the 8C discharging rate at 446 s (Sim, simulation; Exp, experimental).

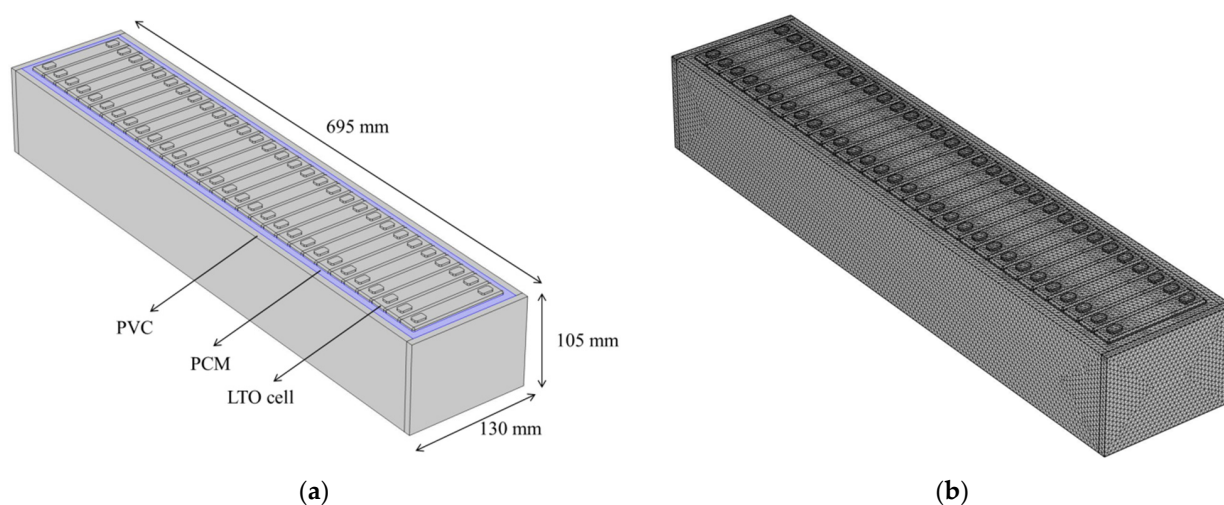## 4. Performance of the Natural Convection, PCM, and PCM-Graphite in Module Level

4.1. Configuration Design of the Module

In the current section, a battery module comprising 30 cells is simulated to describe the thermal effectiveness of the passive cooling strategies comprising natural convection, PCM, and PCM-graphite. Module thermal management needs special attention since cells are affected by each other heat generation during the charging/discharging process. In the current simulation, the module is discharged in a high current profile at 446 s. Active cooling systems are the most common types of cooling systems for the battery module/pack, especially in high current applications. However, in this study, the passive phase change cooling method is used for the thermal management of battery module temperature. The key data of the module are presented in Table 4.

Table 4. The key data of the module adapted from [18].

Parameter	Value
Number of cells in series	30
Nominal voltage of the module (V)	69
Weight (kg)	16.5
Volume (L)	7.8
Stored energy in the module (KWh)	1.6

Figure 8a,b shows the schematic geometry components, dimensions, and mesh distribution of the module, respectively. In the following design, the module consisted of 30 cells which are submerged in PCM and PCM-graphite. The initial temperature of the module, PCM, and the ambient are set at 22 °C. The mesh type is unstructured tetrahedral, which is generated by default physics-controlled mesh in COMSOL Multiphysics®.

(**a**)

(**b**)

Figure 8. (**a**) Schematic of the battery module equipped with PCM and (**b**) mesh distribution.

4.2. Simulation Results

4.2.1. Cooling Effect of Natural Convection, PCM and PCM-Graphite

The initial cooling phase of the battery module is natural convection condition, which can be used as a source to compare with the cooling efficiency of the PCM and PCM-graphite methods. The initial boundary condition for module testing is the same as the cell level. Figure 9 displays the battery module, which cooled through natural convection, PCM, and PCM-graphite that experiences a maximum temperature of 58.8 °C, 49.9 °C, and 48.6 °C, respectively. The limited cooling surface area and the low heat transfer coefficient of the air are the main inabilities of the natural convection cooling method. Moreover, the temperature uniformity is low, with more concentration in the center and top regions of the cells [14]. It is found that the maximum temperature of the module experiences a 15.1% and 17.3% reduction by PCM and PCM-graphite methods, respectively. Moreover, the temperature distribution uniformity has an excellent improvement. Nevertheless, the module temperature can be further improved using more spacing between the cells.
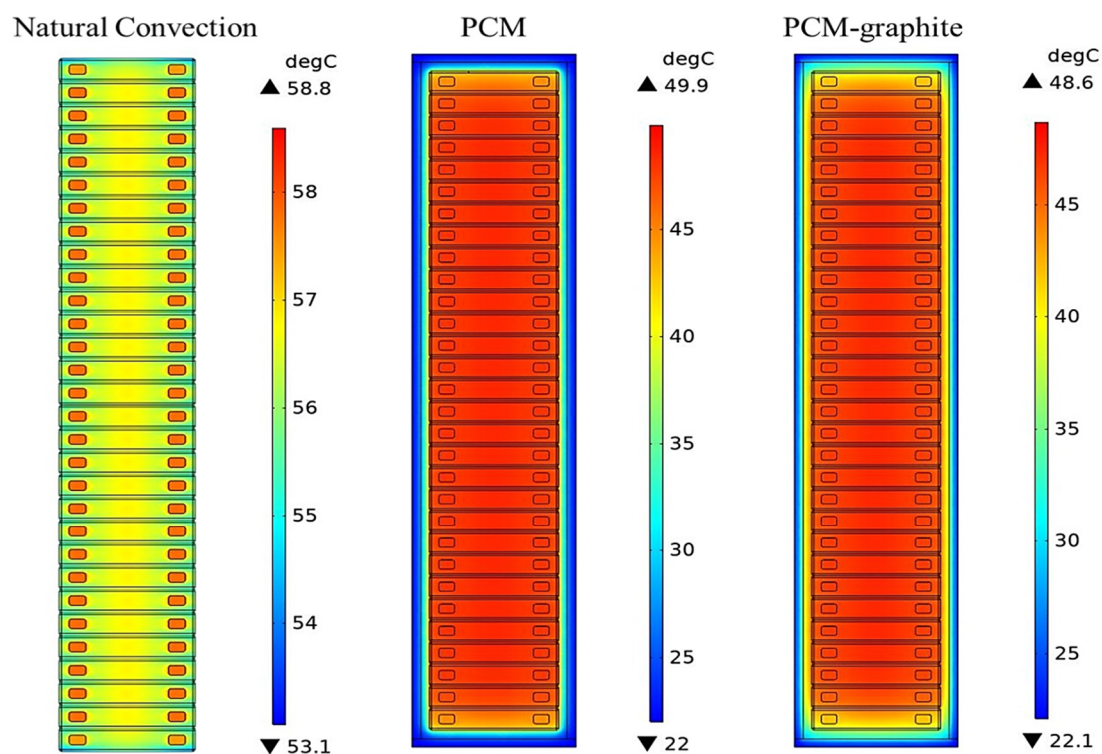
Figure 9. Temperature contour of the battery module in natural convection, PCM, and PCM-graphite under the 8C (184A) discharging rate at 446 s.

4.2.2. Cooling Effect of Cell Spacing Using PCM and PCM-Graphite Methods

The maximum temperature of the cells is a critical problem for any battery module, which can effectively affect the battery's life and capacity. The spacing of the cells is an important element to increase the efficiency of the passive thermal management methods. In the current section, the influence of cell spacing from 0 to 8 mm is considered on the maximum temperature of the module. The appropriate structure and spacing reduce the possibility of battery thermal runaway. Table 5 summarizes the simulation results about the effects of the spacing on the maximum temperature of the battery module. It can be seen the maximum temperature of the module for 8 mm spacing reaches 43.4 °C and 41.9 °C, which results in 13% and 13.7% temperature reduction for PCM and PCM-graphite cooling methods, respectively.

Table 5. Cell spacing effect of the battery module.

Spacing (Cells)	Module Temperature (PCM)	Module Temperature (PCM-Graphite)	Temperature Reduction (PCM)	Temperature Reduction (PCM-Graphite)	Energy Density (Wh/L)
0 mm	49.9 °C	48.6 °C	-	-	659.2
2 mm	47.5 °C	46.4 °C	4.8%	4.5%	608.7
4 mm	45.7 °C	44.6 °C	8.4%	8.2%	565.5
6 mm	44.4 °C	43.1 °C	11%	11.3%	528
8 mm	43.4 °C	41.9 °C	13%	13.7%	495.1

5. Conclusions

The experimental and numerical studies were performed to investigate the cooling performance of different passive TMSs for the LTO cell/module in a high current discharging process. In the same initial conditions, the average temperature of the cell in lack of natural convection, natural convection, Al mesh, Cu mesh, PCM, and PCM-graphite

reaches the 57.2 °C, 53.5 °C, 52.9 °C, 52.2 °C, 39.9 °C, and 34.71 °C, respectively. It is found experimentally that PCM and PCM-graphite cooling methods are preserved the battery temperature in a safe temperature zone. In the simulation section, the cooling effect of natural convection, PCM, and PCM-graphite are considered at the module level. The numerical results are validated with the experimental results in an acceptable agreement.

According to the results, there is a 15.1% and 17.3% reduction in maximum module temperature by PCM and PCM-graphite methods, respectively. Moreover, the results exhibit that cell spacing has an enormous impact on the temperature reduction of the module. The maximum temperature of the module for 8 mm spacing reaches 43.4 °C and 41.9 °C, which results in 13% and 13.7% temperature reduction for PCM and PCM-graphite cooling methods, respectively.

6. Future Work

Utilizing passive cooling methods like PCM cooling systems can be an effective way for battery thermal management applications. However, most PCMs suffer from low thermal conductivity. Therefore, using more additive materials like nanoparticles, carbon nanotube, heat pipe, fin in different percentages and configurations can be studied for the next step in pack level.

Author Contributions: Conceptualization, methodology, software, validation, formal analysis, investigation, writing—original journal draft by H.B., writing, review & Editing by D.K., R.Y., M.S.P., J.V.M., supervision, writing—review & editing by M.B. All authors have read and agreed to the published version of the manuscript.

Conflicts of Interest: The authors declare no conflict of interest.

References

1. Mirmohammadi, S.A.; Behi, M.R.; Suma, A.B.; Palm, B.E. Multi-Criteria Analysis, Evaluation and Modeling of Future Scenario for the Energy Generation Sector—A Case Study. In Proceedings of the ASME 2014 Power Conference, Baltimore, MD, USA, 28–31 July 2014. [CrossRef]
2. Ghezelbash, R.; Farzaneh-Gord, M.; Behi, H.; Sadi, M.; Khorramabady, H.S. Performance assessment of a natural gas expansion plant integrated with a vertical ground-coupled heat pump. *Energy* **2015**, *93*, 2503–2517. [CrossRef]
3. Feng, X.; Zheng, S.; Ren, D.; He, X.; Wang, L.; Cui, H.; Liu, X.; Jin, C.; Zhang, F.; Xu, C.; et al. Investigating the thermal runaway mechanisms of lithium-ion batteries based on thermal analysis database. *Appl. Energy* **2019**, *246*, 53–64. [CrossRef]
4. Khaleghi, S.; Karimi, D.; Beheshti, S.H.; Hosen, M.S.; Behi, H.; Berecibar, M.; van Mierlo, J. Online health diagnosis of lithium-ion batteries based on nonlinear autoregressive neural network. *Appl. Energy* **2021**, *282*, 116159. [CrossRef]
5. Karimi, D.; Behi, H.; Jaguemont, J.; Berecibar, M.; van Mierlo, J. A refrigerant-based thermal management system for a fast charging process for lithium-ion batteries. In Proceedings of the International Conference on Renewable Energy Systems and Environmental Engineering, Brussels, Brussels, Belgium, 17–18 December 2020; Global Publisher: Brussels, Belgium, 2020; pp. 1–6.
6. Karimi, D.; Khaleghi, S.; Behi, H.; Beheshti, H.; Hosen, M.S.; Akbarzadeh, M.; van Mierlo, J.; Berecibar, M. Lithium-Ion Capacitor Lifetime Extension through an Optimal Thermal Management System for Smart Grid Applications. *Energies* **2021**, *14*, 2907. [CrossRef]
7. Saw, L.H.; Ye, Y.; Tay, A.A.O.; Chong, W.T.; Kuan, S.H.; Yew, M.C. Computational fluid dynamic and thermal analysis of Lithium-ion battery pack with air cooling. *Appl. Energy.* **2016**, *177*, 783–792. [CrossRef]
8. Yahyaie, A.; Mirmohammadi, S.A.A.; Behi, M.R.; Sadi, M.; Behi, H.R. Theoretical investigation on producing work by applying different refrigerants in typical power cycle. In Proceedings of the Scientific Society of Measurement, Automation and Informatics, Branch of Thermal Engineering and Thermogrammetry, Budapest, Hungary, 1–3 July 2009. Available online: http://inis.iaea.org/search/search.aspx?orig_q=RN:40102982.03.07.2009 (accessed on 31 May 2021).

9. Behi, H. Experimental and Numerical Study on Heat Pipe Assisted PCM Storage System. Master's Thesis, Royal Institute of Technology, Stockholm, Sweden, 2015. Available online: http://www.diva-portal.org/smash/get/diva2:850104/FULLTEXT01.pdf (accessed on 30 May 2021).

10. Behi, M.; Mirmohammadi, S.A.; Ghanbarpour, M.; Behi, H.; Palm, B. Evaluation of a novel solar driven sorption cooling/heating system integrated with PCM storage compartment. *Energy* **2018**, *164*, 449–464. [CrossRef]

11. Behi, H.; Karimi, D.; Jaguemont, J.; Gandoman, F.H.; Khaleghi, S.; van Mierlo, J.; Berecibar, M. Aluminum Heat Sink Assisted Air-Cooling Thermal Management System for High Current Applications in Electric Vehicles. In Proceedings of the 2020 AEIT International Conference of Electrical and Electronic Technologies for Automotive (AEIT AUTOMOTIVE), Turin, Italy, 18–20 November 2020; pp. 1–6.

12. Mirmohammadi, S.A.; Behi, M.; Ghanbarpour, M. Cooling performance study of a novel heat exchanger in an absorption system. *Energy Convers. Manag.* **2019**, *180*, 1001–1012. [CrossRef]

13. Behi, H.; Ghanbarpour, M.; Behi, M. Investigation of PCM-assisted heat pipe for electronic cooling. *Appl. Therm. Eng.* **2017**, *127*, 1132–1142. [CrossRef]

14. Behi, H.; Karimi, D.; Behi, M.; Jaguemont, J.; Ghanbarpour, M.; Behnia, M.; Berecibar, M.; van Mierlo, J. Thermal management analysis using heat pipe in the high current discharging of lithium-ion battery in electric vehicles. *J. Energy Storage* **2020**, *32*, 101893. [CrossRef]

15. Behi, H.; Karimi, D.; Jaguemont, J.; Berecibar, M.; van Mierlo, J. Experimental study on cooling performance of flat heat pipe for lithium-ion battery at various inclination angels. *Energy Perspect.* **2020**, *1*, 77–92.

16. Behi, H.; Karimi, D.; Behi, M.; Ghanbarpour, M.; Jaguemont, J.; Sokkeh, M.A.; Gandoman, F.H.; Berecibar, M.; van Mierlo, J. A new concept of thermal management system in Li-ion battery using air cooling and heat pipe for electric vehicles. *Appl. Therm. Eng.* **2020**, *174*, 115280. [CrossRef]

17. Behi, H.; Behi, M.; Karimi, D.; Jaguemont, J.; Ghanbarpour, M.; Behnia, M.; Berecibar, M.; van Mierlo, J. Heat pipe air-cooled thermal management system for lithium-ion batteries: High power applications. *Appl. Therm. Eng.* **2020**, *183*, 116240. [CrossRef]

18. Behi, H.; Karimi, D.; Jaguemont, J.; Gandoman, F.H.; Kalogiannis, T.; Berecibar, M.; van Mierlo, J. Novel thermal management methods to improve the performance of the Li-ion batteries in high discharge current applications. *Energy* **2021**, *224*, 120165. [CrossRef]

19. Karimi, D.; Behi, H.; Jaguemont, J.; Berecibar, M.; van Mierlo, J. Investigation of extruded heat sink assisted air cooling system for lithium-ion capacitor batteries. In Proceedings of the International Conference on Renewable Energy Systems and Environmental Engineering, Brussels, Belgium, 17–18 December 2020; Global Publisher: Brussels, Belgium, 2020; pp. 1–6.

20. Karimi, D.; Behi, H.; Jaguemont, J.; Berecibar, M.; van Mierlo, J. Optimized air-cooling thermal management system for high power lithium-ion capacitors. *Energy* **2020**. Available online: http://globalpublisher.org/journals-1006/ (accessed on 31 May 2021).

21. Wang, H.; Tao, T.; Xu, J.; Mei, X.; Liu, X.; Gou, P. Cooling capacity of a novel modular liquid-cooled battery thermal management system for cylindrical lithium ion batteries. *Appl. Therm. Eng.* **2020**, *178*, 115591. [CrossRef]

22. Karimi, D.; Behi, H.; Jaguemont, J.; el Baghdadi, M.; van Mierlo, J.; Hegazy, O. Thermal Concept Design of MOSFET Power Modules in Inverter Subsystems for Electric Vehicles, In Proceedings of the 2019 9th International Conference on Power and Energy Systems (ICPES), Perth, WA, Australia, 10–12 December 2019.

23. Karimi, D.; Behi, H.; Hosen, M.S.; Jaguemont, J.; Berecibar, M.; van Mierlo, J. A compact and optimized liquid-cooled thermal management system for high power lithium-ion capacitors. *Appl. Therm. Eng.* **2021**, *185*, 116449. [CrossRef]

24. Gandoman, F.H.; Behi, H.; Berecibar, M.; Jaguemont, J.; Aleem, S.H.E.A.; Behi, M.; van Mierlo, J. Chapter 16—Reliability evaluation of Li-ion batteries for electric vehicles applications from the thermal perspectives. In *Uncertainties in Modern Power Systems*; Zobaa, A.F., Aleem, S.H.E.A., Eds.; Academic Press: Cambridge, MA, USA, 2021; pp. 563–587. [CrossRef]

25. Karimi, D.; Jaguemont, J.; Behi, H.; Berecibar, M.; van den Bossche, P.; van Mierlo, J. Passive cooling based battery thermal management using phase change materials for electric vehicles. In Proceedings of the EVS33 International Electric Vehicle Symposium, Portland, OR, USA, 14–17 June 2020; The Electric Drive Transportation Association EDTA: Portland, OR, USA, 2020.

26. Heyhat, M.M.; Mousavi, S.; Siavashi, M. Battery thermal management with thermal energy storage composites of PCM, metal foam, fin and nanoparticle. *J. Energy Storage* **2020**, *28*, 101235. [CrossRef]

27. Behi, M.; Shakorian-poor, M.; Mirmohammadi, S.A.; Behi, H.; Rubio, J.I.; Nikkam, N.; Farzaneh-Gord, M.; Gan, Y.; Behnia, M. Experimental and numerical investigation on hydrothermal performance of nanofluids in micro-tubes. *Energy* **2020**, *193*, 116658. [CrossRef]

28. Mirmohammadi, S.; Behi, M. Investigation on Thermal Conductivity, Viscosity and Stability of Nanofluids. 2012. Available online: http://kth.diva-portal.org/smash/record.jsf?pid=diva2:537164 (accessed on 30 May 2021).

29. Mirmohammadi, S.A.; Behi, M.; Gan, Y.; Shen, L. Particle-shape-, temperature-, and concentration-dependent thermal conductivity and viscosity of nanofluids. *Phys. Rev. E* **2019**, *99*, 43109. [CrossRef] [PubMed]

30. Karimi, D.; Behi, H.; Jaguemont, J.; Sokkeh, M.A.; Kalogiannis, T.; Hosen, M.S.; Berecibar, M.; van Mierlo, J. Thermal performance enhancement of phase change material using aluminum-mesh grid foil for lithium-capacitor modules. *J. Energy Storage* **2020**, *30*, 101508. [CrossRef]

31. Jaguemont, J.; Karimi, D.; van Mierlo, J. Investigation of a passive thermal management system for lithium-ion capacitors. *IEEE Trans. Veh. Technol.* **2019**, *68*, 1. [CrossRef]

32. Al Hallaj, S.; Selman, J.R. A novel thermal management system for electric vehicle batteries using phase-change material. *J. Electrochem. Soc.* **2000**, *147*, 3231. [CrossRef]

33. Babapoor, A.; Azizi, M.; Karimi, G. Thermal management of a Li-ion battery using carbon fiber-PCM composites. *Appl. Therm. Eng.* **2015**, *82*, 281–290. [CrossRef]

34. Wang, W.; Zhang, X.; Xin, C.; Rao, Z. An experimental study on thermal management of lithium ion battery packs using an improved passive method. *Appl. Therm. Eng.* **2018**, *134*, 163–170. [CrossRef]

35. Huang, Q.; Li, X.; Zhang, G.; Zhang, J.; He, F.; Li, Y. Experimental investigation of the thermal performance of heat pipe assisted phase change material for battery thermal management system. *Appl. Therm. Eng.* **2018**, *141*, 1092–1100. [CrossRef]

36. Weng, J.; Ouyang, D.; Yang, X.; Chen, M.; Zhang, G.; Wang, J. Optimization of the internal fin in a phase-change-material module for battery thermal management. *Appl. Therm. Eng.* **2020**, *167*, 114698. [CrossRef]

37. Behi, H.; Karimi, D.; Gandoman, F.H.; Akbarzadeh, M.; Khaleghi, S.; Kalogiannis, T.; Hosen, M.S.; Jaguemont, J.; van Mierlo, J.; Berecibar, M. PCM assisted heat pipe cooling system for the thermal management of an LTO cell for high-current profiles. *Case Stud. Therm. Eng.* **2021**, *25*, 100920. [CrossRef]

38. El Idi, M.M.; Karkri, M.; Tankari, M.A. A passive thermal management system of Li-ion batteries using PCM composites: Experimental and numerical investigations. *Int. J. Heat Mass Transf.* **2021**, *169*, 120894. [CrossRef]

39. Wu, W.; Yang, X.; Zhang, G.; Chen, K.; Wang, S. Experimental investigation on the thermal performance of heat pipe-assisted phase change material based battery thermal management system. *Energy Convers. Manag.* **2017**, *138*, 486–492. [CrossRef]

40. Samimi, F.; Babapoor, A.; Azizi, M.; Karimi, G. Thermal management analysis of a Li-ion battery cell using phase change material loaded with carbon fibers. *Energy* **2016**, *96*, 355–371. [CrossRef]

41. Behi, M.; Mirmohammadi, S.A.; Suma, A.B.; Palm, B.E. Optimized Energy Recovery in Line with Balancing of an ATES. In Proceedings of the ASME 2014 Power Conference, Baltimore, MD, USA, 28–31 July 2014. [CrossRef]

42. Liu, L.; Zhu, L.; Wang, Y.; Huang, Q.; Sun, Y.; Yin, Z. Heat dissipation performance of silicon solar cells by direct dielectric liquid immersion under intensified illuminations. *Sol. Energy* **2011**, *85*, 922–930. [CrossRef]

43. Hosen, M.S.; Karimi, D.; Kalogiannis, T.; Pirooz, A.; Jaguemont, J.; Berecibar, M.; van Mierlo, J. Electro-aging model development of nickel-manganese-cobalt lithium-ion technology validated with light and heavy-duty real-life profiles. *J. Energy Storage* **2020**, *28*, 101265. [CrossRef]

44. Soltani, M.; Ronsmans, J.; Jaguemont, J.; van Mierlo, J.; van den Bossche, P.; Omar, N. A Three-dimensional thermal model for a commercial lithium-ion capacitor battery pack with non-uniform temperature distribution. In Proceedings of the 2019 IEEE International Conference on Industrial Technology (ICIT), Melbourne, VIC, Australia, 13–15 February 2019; pp. 1126–1131. [CrossRef]

45. Jaguemont, J.; Boulon, L.; Dubé, Y. Characterization and modeling of a hybrid-electric-vehicle lithium-ion battery pack at low temperatures. *IEEE Trans. Veh. Technol.* **2016**, *65*, 1–14. [CrossRef]

46. Akbarzadeh, M.; Jaguemont, J.; Kalogiannis, T.; Karimi, D.; He, J.; Jin, L.; Xie, P.; van Mierlo, J.; Berecibar, M. A novel liquid cooling plate concept for thermal management of lithium-ion batteries in electric vehicles. *Energy Convers. Manag.* **2021**, *231*, 113862. [CrossRef]

47. Zhao, L.; Wang, J.; Li, Y.; Liu, Q.; Li, W. Experimental investigation of a lithium battery cooling system. *Sustainability* **2019**, *11*, 5020. [CrossRef]